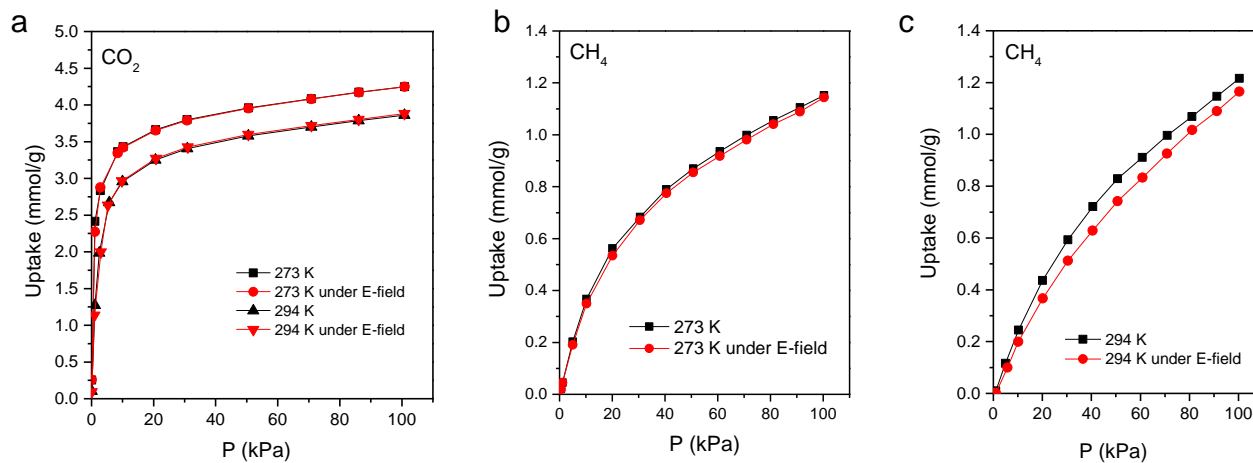


Supplementary Information

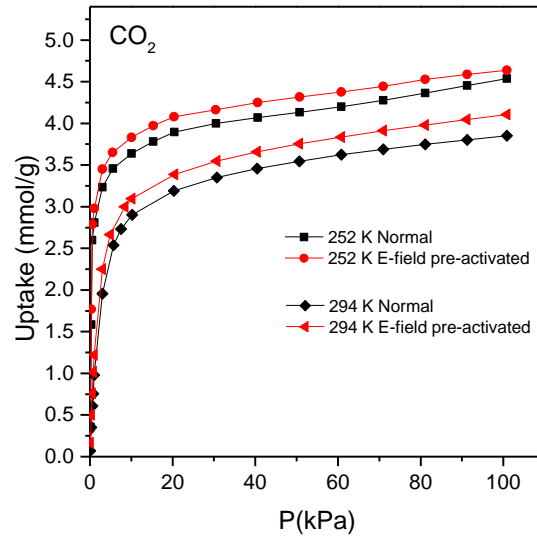
Regulating Adsorption Performance of Zeolites by Pre-activation in Electric Fields

Kaifei Chen et al.

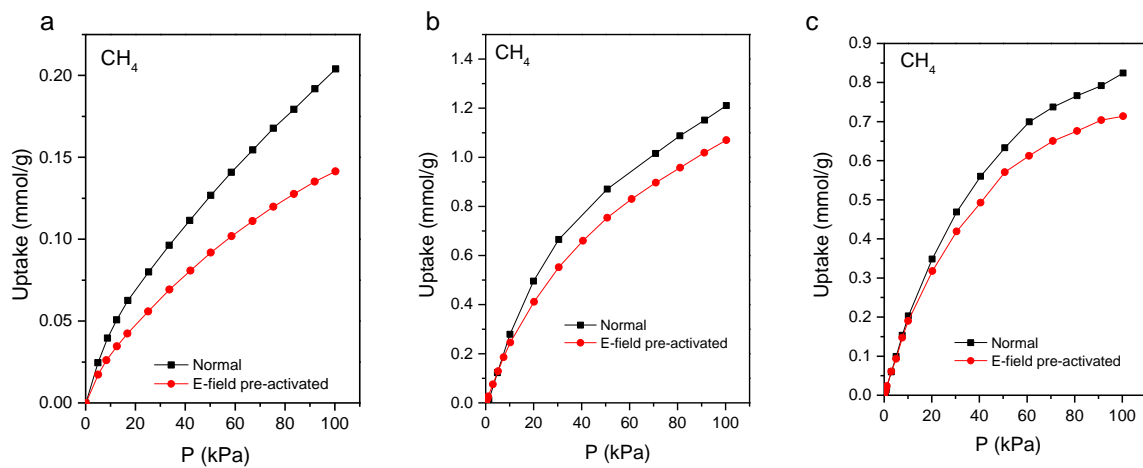
Supplementary Figures



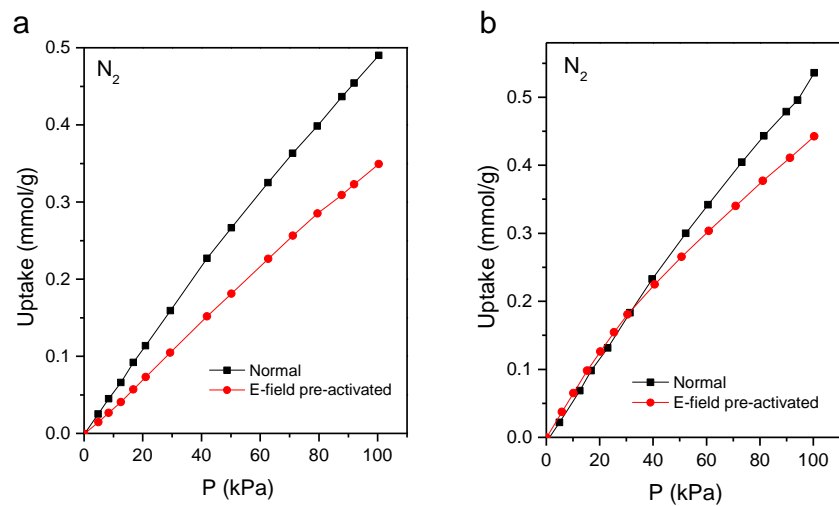
Supplementary Figure 1 Adsorption isotherms of (a) CO₂ and (b-c) CH₄ at 273 K and 294 K in r2KCHA without or with the *in situ* application of a 240 V/mm E-field.



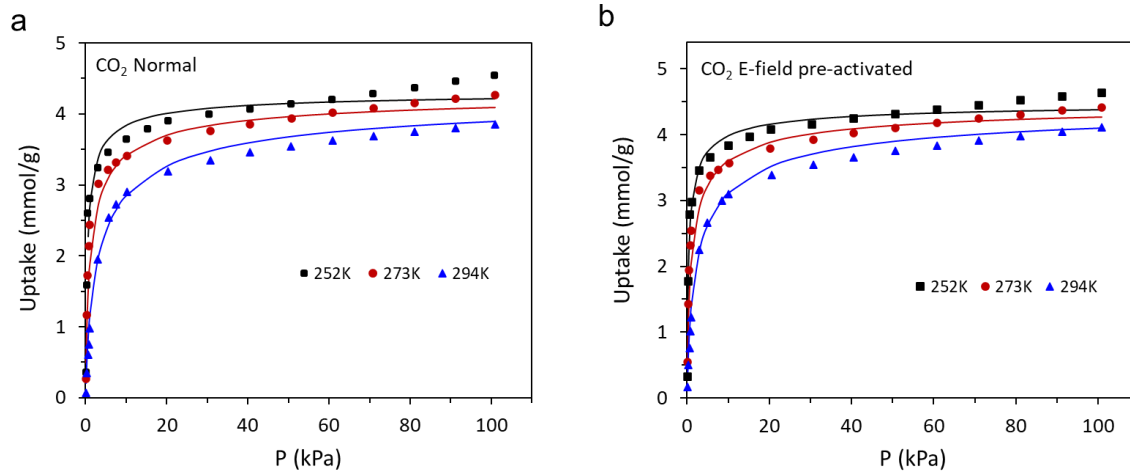
Supplementary Figure 2 Adsorption isotherms of CO₂ in r2KCHA at 252 K and 294 K without and with the E-field pre-activation.



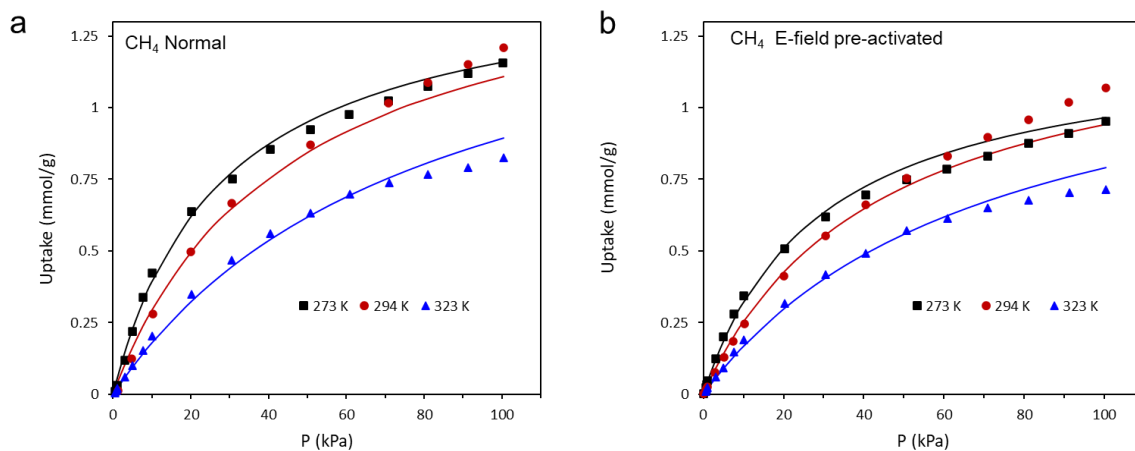
Supplementary Figure 3 Adsorption isotherms of CH₄ in r2KCHA at (a) 252 K, (b) 294 K and (c) 323 K without and with the E-field pre-activation. Because of the trapdoor effect, the uptakes of CH₄ at 273 and 294 K were close, leading to a crossover of the isotherms.



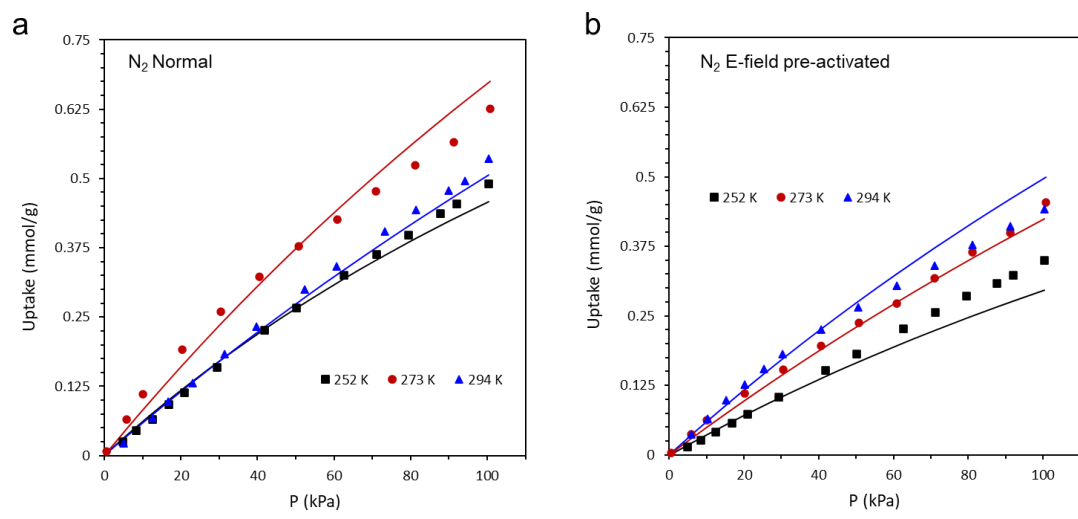
Supplementary Figure 4 Adsorption isotherms of N_2 in r2KCHA at (a) 252 K and (b) 294 K without and with the E-field pre-activation.



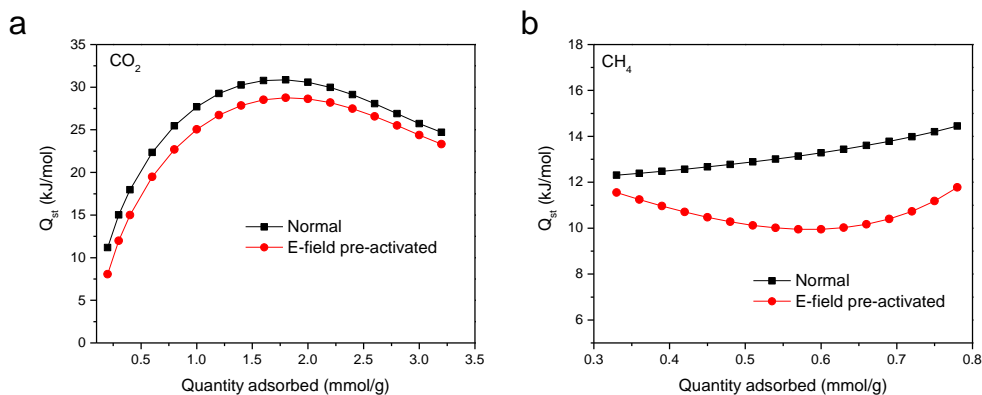
Supplementary Figure 5 Adsorption isotherms of CO₂ in r2KCHA fitted with Toth model (a) without and (b) with the E-field pre-activation. Solid symbols refer to the experimental data, with curves depicting the theoretical-fitting results using the Toth model.



Supplementary Figure 6 Adsorption isotherms of CH₄ in r2KCHA fitted with LJM-Toth model (a) without and (b) with the E-field pre-activation. Solid symbols refer to the experimental data, with curves depicting the theoretical-fitting results using the LJM-Toth model.



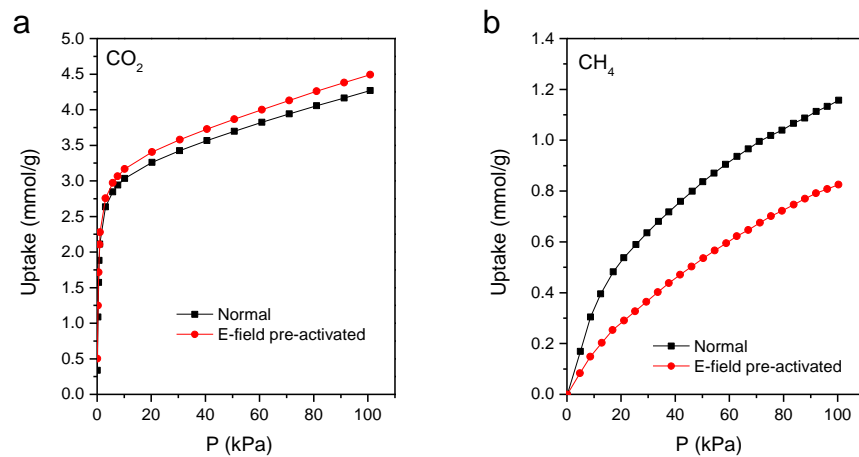
Supplementary Figure 7 Adsorption isotherms of N₂ in r2KCHA fitted with LJM-Toth model (a) without and (b) with the E-field pre-activation. Solid symbols refer to the experimental data with curves depicting the theoretical-fitting results using the LJM-Toth model.



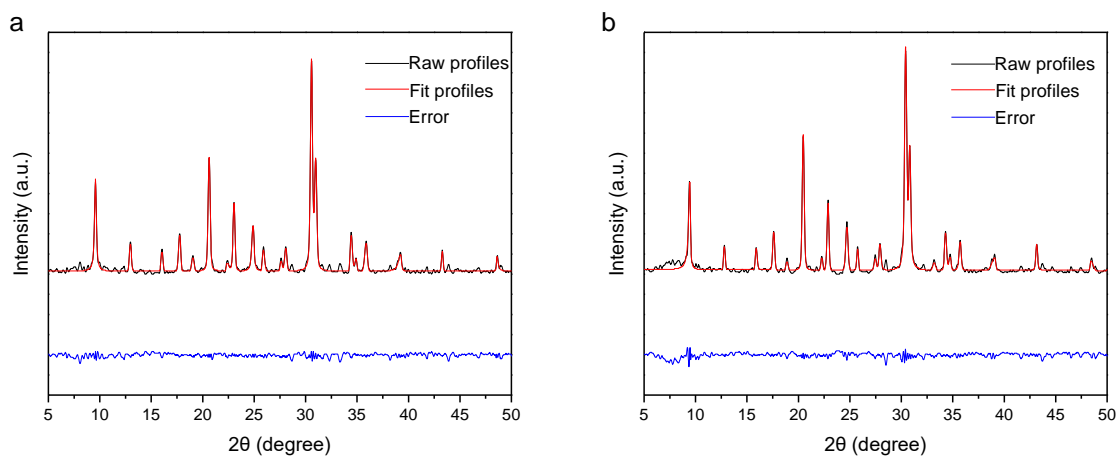
Supplementary Figure 8 The isosteric heat of adsorption Q_{st} of (a) CO₂ and (b) CH₄ in r2KCHA before and after the E-field pre-activation. The Q_{st} of CO₂ was calculated in the temperature range of 252 K to 294 K. The Q_{st} of CH₄ was calculated in the temperature range of 273 K to 323 K to avoid the influence of the trapdoor effect.

The heat of adsorption curve of CO₂ was first increased at the low coverage, which might be resulted from the strong interaction of the trapdoor cation and the CO₂ molecule at the beginning of adsorption. After a certain coverage, the increase of adsorbate–adsorbate interaction energy was limited by the adsorption capacity, while the drop of field gradient–quadrupole interaction, dispersion energy, repulsion energy, and polarization energy became dominant, finally leading to a decline in the Q_{st} .¹

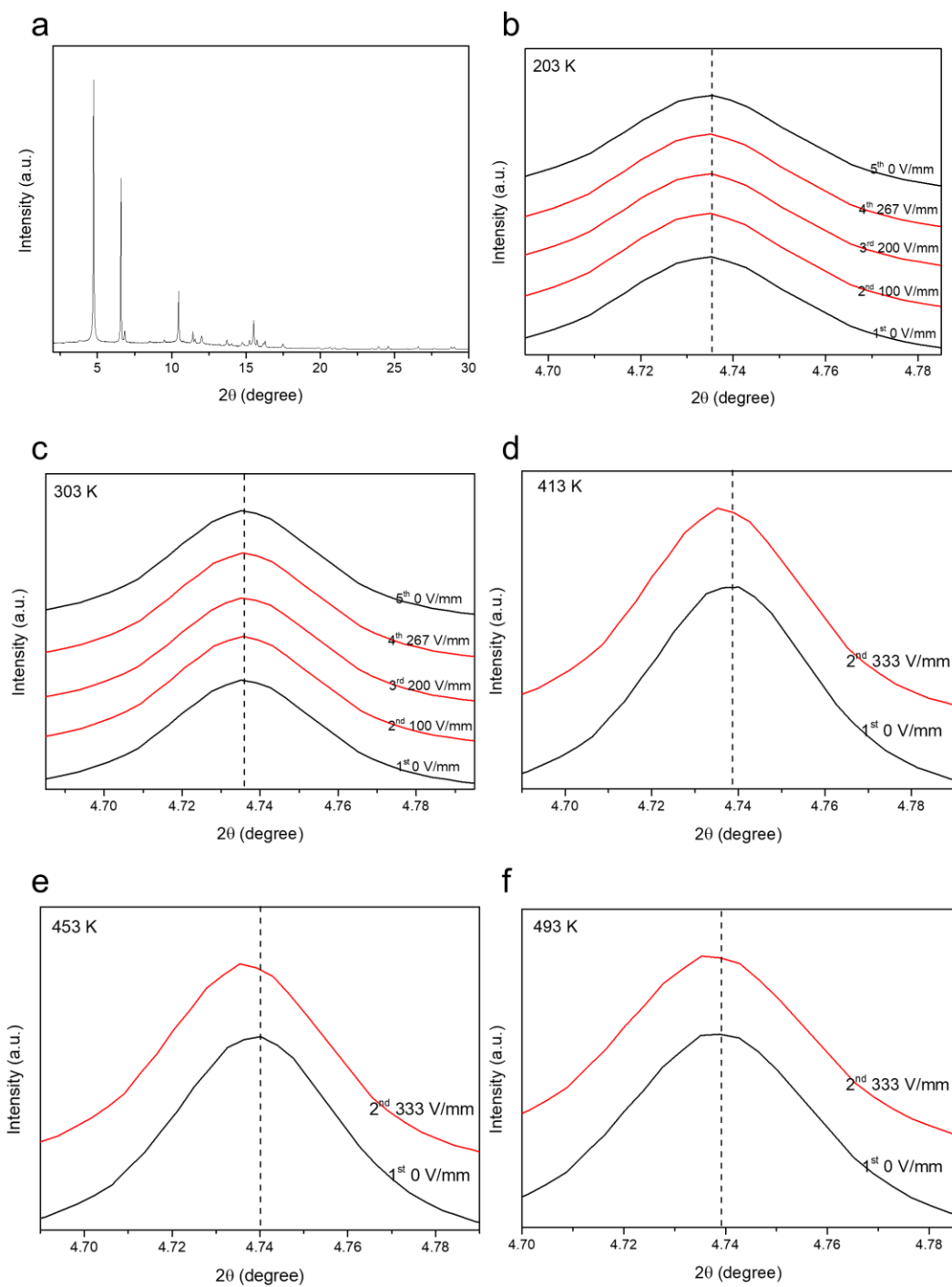
The heat of adsorption curve of CH₄ in a normal r2KCHA showed a slight increase with increasing coverage. However, after the E-field pre-activation, due to the reduced cation–molecule interaction caused by the relocation of partial K⁺ in the pore, the Q_{st} of CH₄ in r2KCHA exhibited a declining trend at low coverages.



Supplementary Figure 9 Adsorption isotherms of (a) CO₂ and (b) CH₄ in r2KCHA at 273 K without and with the pre-activation of a direct current E-field at the intensity of 800 V/mm.

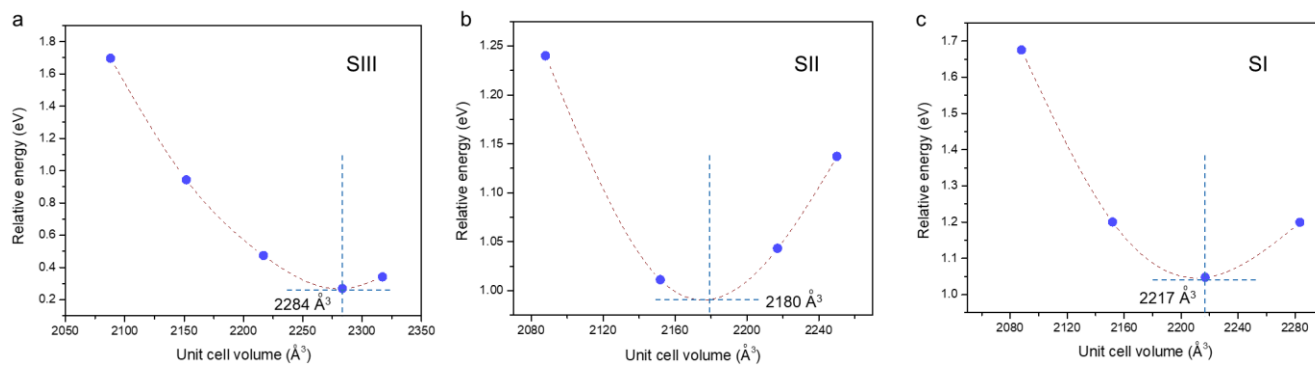


Supplementary Figure 10 PXRD patterns of r2KCHA and the fitted profiles calculated by MDI Jade 6.0. (a) The normal r2KCHA. (b) The E-field pre-activated r2KCHA.

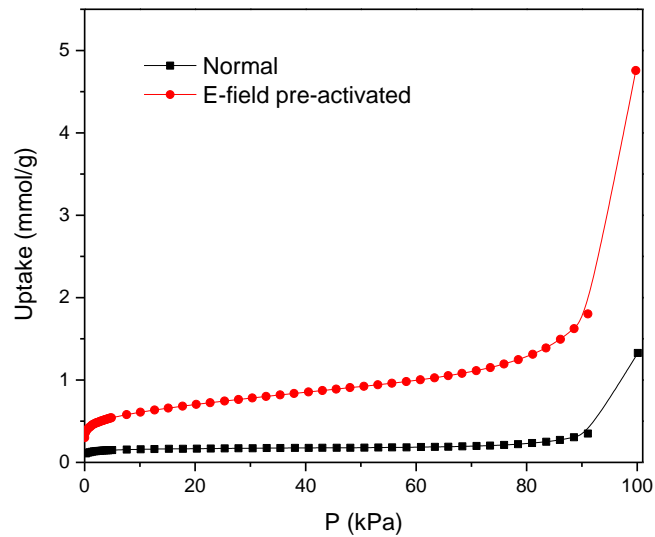


Supplementary Figure 11 Synchrotron PXRD measurements with the *in situ* E-field applications. (a) The complete PXRD pattern of r2KCHA. (b-f) PXRD patterns of r2KCHA with *in situ* E-field applications at (b) 203 K, (c) 303 K, (d) 413 K, (e) 453 K and (f) 493 K. The E-field intensity was 100, 200, 267 and 333 V/mm when the voltage was 120, 240, 320 V and

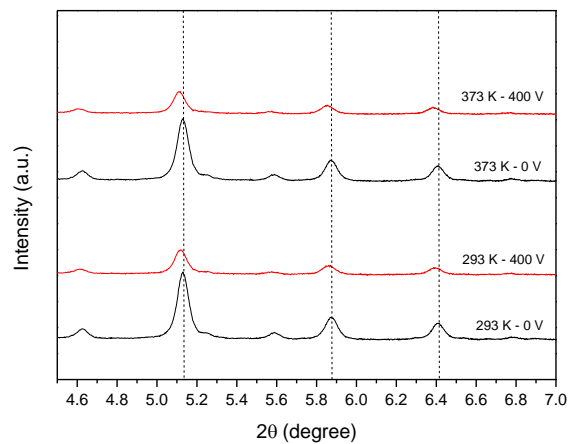
400 V respectively. At 203 and 303 K, the r2KCHA sample was successively exposed to the E-fields of 0, 100, 200, 267 and 0 V/mm. At 413, 453 and 493 K, the r2KCHA sample was successively exposed to the E-fields of 0 and 333 V/mm.



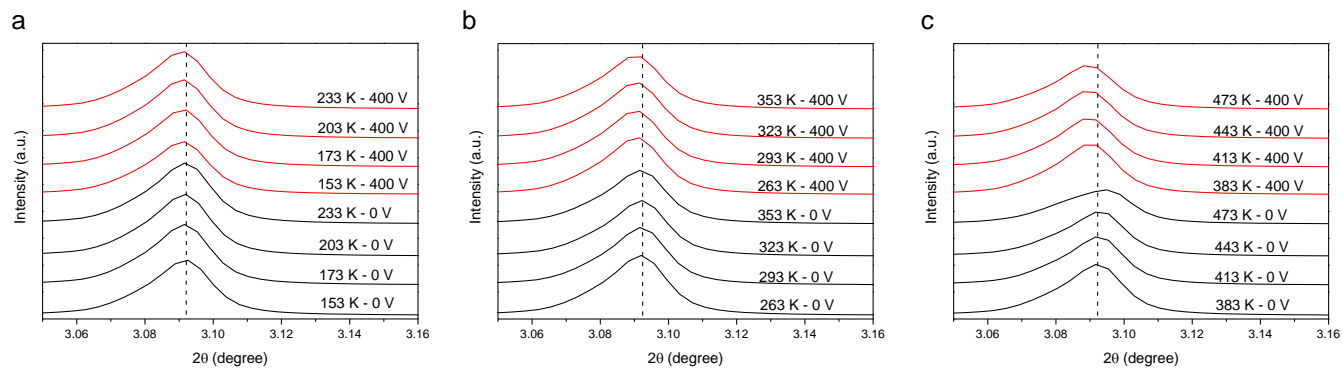
Supplementary Figure 12 Changes of relative energy over unit cell volume of r2KCHA with one K^+ moving from SIII' to (a) SIII, (b) SII and (c) SI.



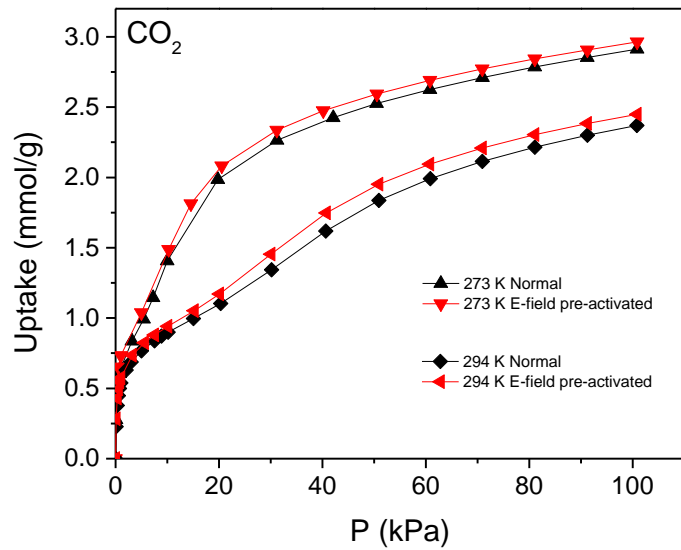
Supplementary Figure 13 Adsorption isotherms of N₂ in r2KCHA at 77 K without and with the E-field pre-activation.



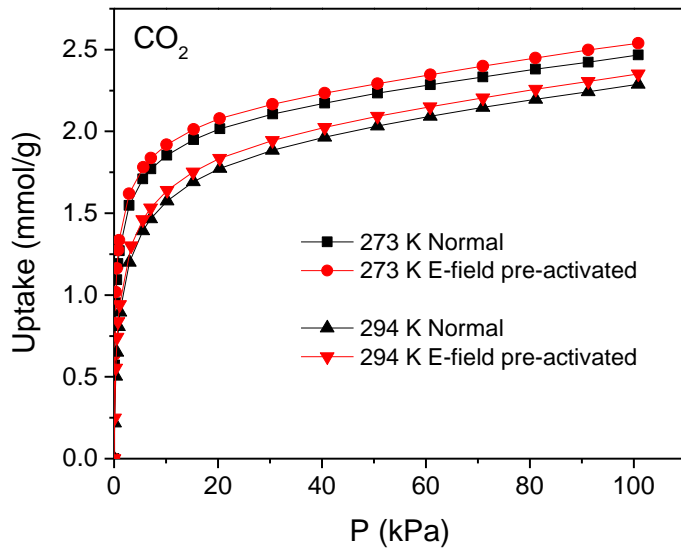
Supplementary Figure 14 Synchrotron PXRD analysis of ZSM-25-K under vacuum with *in situ* application of the E-field at 293 and 373 K. The E-field intensity was 200 V/mm when the voltage was 400 V. The X-ray wavelength was 0.6888 Å.



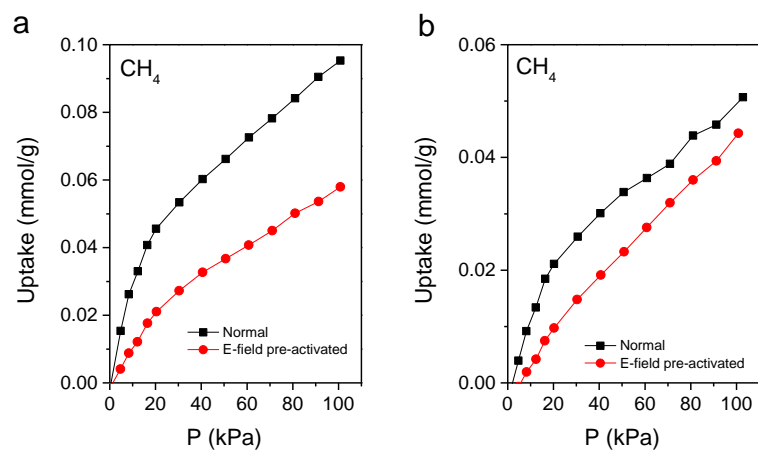
Supplementary Figure 15 Synchrotron PXRD analysis of TMA-Y under vacuum with *in situ* application of the E-field at (a) 153-233 K, (b) 263-353 K and (c) at 383-473 K. The E-field intensity was 333 V/mm when the voltage was 400 V. The X-ray wavelength was 0.7732 Å.



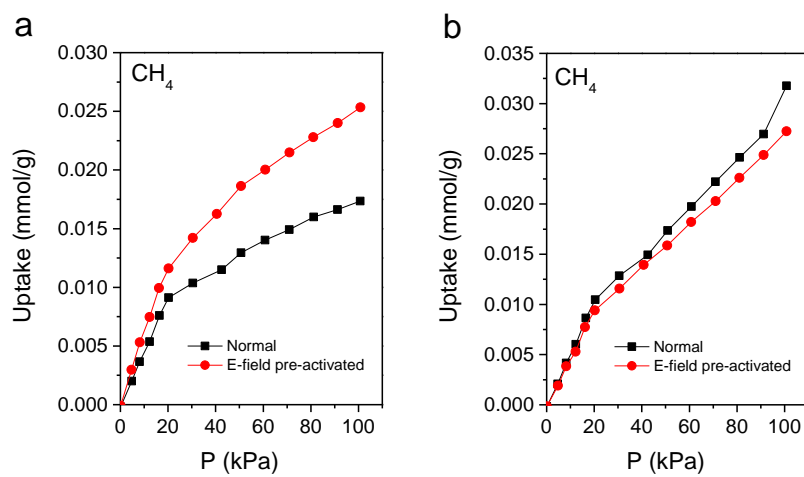
Supplementary Figure 16 Adsorption isotherms of CO₂ in ZSM-25-Na at 273 K and 294 K without and with the E-field pre-activation. The Na-ZSM-25 exhibited a rapid increase of CO₂ uptake at low pressures and a flat upward trend at high pressures, which was attributed to the framework expansion while adsorbing CO₂.²



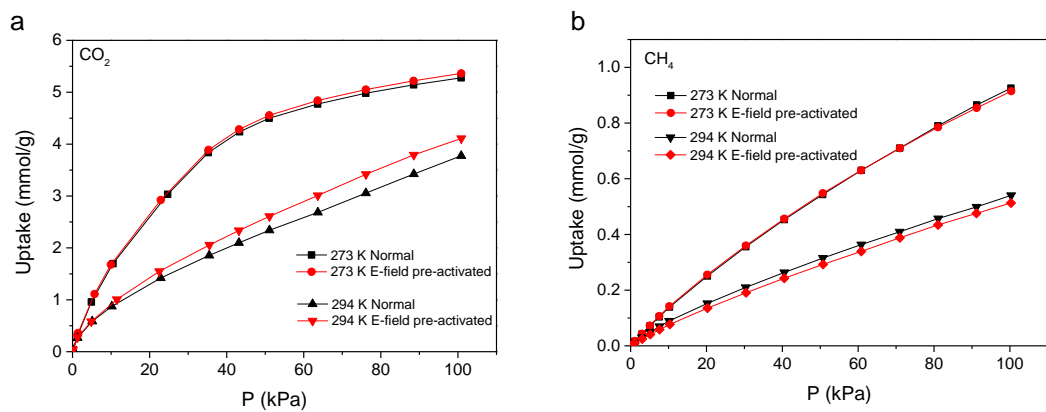
Supplementary Figure 17 Adsorption isotherms of CO₂ in ZSM-25-K at 273 K and 294 K without and with the E-field pre-activation.



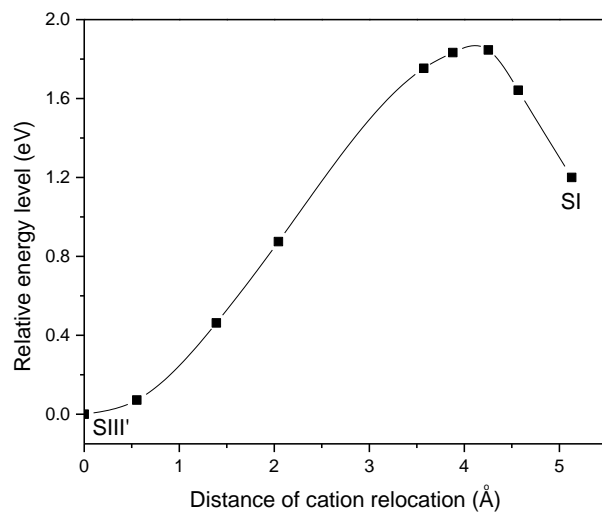
Supplementary Figure 18 Adsorption isotherms of CH₄ in ZSM-25-Na at (a) 273 K and (b) 294 K and without and with the E-field pre-activation.



Supplementary Figure 19 Adsorption isotherms of CH₄ in ZSM-25-K at (a) 273 K and (b) 294 K without and with the E-field pre-activation.



Supplementary Figure 20 Adsorption isotherms of (a) CO₂ and (b) CH₄ in TMA-Y without and with the E-field pre-activation.



Supplementary Figure 21 The energy profile for one K^+ in r2KCHA relocating between SIII' and SI calculated by DFT.

Supplementary Tables

Supplementary Table 1 Parameters of CO₂ adsorption isotherms of r2KCHA fitted with Toth model

	q_m (mol kg ⁻¹)	K^0	Q (kJ/mol)	t
Normal	4.34	2.05E-06	30.9	0.64
E-field pre-activated	4.53	9.76E-06	28.0	0.61

	T (K)	R ²
	252	0.95
Normal	273	0.96
	294	0.99
	252	0.95
E-field pre-activated	273	0.97
	294	0.99

Supplementary Table 2 Parameters of CH₄ adsorption isotherms of r2KCHA fitted with LJM-Toth model

	q _m (mol kg ⁻¹)	K ⁰	Q (kJ/mol)	t
Normal	1.62	3.90E-05	15.5	0.98
E-field pre-activated	1.35	1.05E-04	13.2	0.99

	T (K)	R ²
	273	0.99
Normal	294	0.99
	323	0.99
	273	0.99
E-field pre-activated	294	0.98
	323	0.99

Supplementary Table 3 Parameters of N₂ adsorption isotherms of r2KCHA fitted with LJM-Toth model

	q _m (mol kg ⁻¹)	K ⁰	Q (kJ/mol)	t
Normal	3.32	2.00E-05	11.0	0.99
E-field pre-activated	2.71	1.58E-04	6.02	0.99

	T (K)	R ²
	252	0.99
Normal	273	0.98
	294	0.99
	252	0.95
E-field pre-activated	273	0.93
	294	0.97

Supplementary Notes

Supplementary Note 1: The adsorption models used for the fit of adsorption isotherms of r2KCHA

The adsorption isotherms of CO₂ were fitted with the Toth model³ as described in Equations (S1) and (S2),

$$q = q_m \frac{KP}{[1+(KP)^t]^{1/t}} \quad (\text{S1})$$

$$K = K^0 \cdot \exp\left(-\frac{Q}{RT}\right) \quad (\text{S2})$$

where q and q_m are the absolute adsorbed amount and the maximum adsorbed amount respectively (mol kg⁻¹), P is the pressure (kPa) for loading q , K^0 is the infinite adsorption constant, Q is the isosteric heat of adsorption at zero loading (kJ mol⁻¹), t is the heterogeneity parameter, T is the temperature of the system (K), and R is the gas constant (kJ kg⁻¹ K⁻¹).

The adsorption isotherms of CH₄ and N₂ were fitted with the LJM-Toth model⁴ in Equation (S3), which incorporated new parameters into classical adsorption models to describe the temperature-dependent pore accessibility of trapdoor materials.

$$q = [\Phi(1 - \varepsilon) + \varepsilon] \frac{q_m KP}{[1+(KP)^t]^{1/t}} \quad (\text{S3})$$

In Equation (S3), Φ is the temperature-dependent distribution function and ε is the fraction of external surface sites and defects always available for adsorption. The function $[\Phi(1 - \varepsilon) + \varepsilon]$ determines the fraction of accessible adsorption sites at different temperatures, which is known as site accessibility. Based on the previous studies⁴, the site accessibility of r2KCHA for CH₄ is 0.92 at 273 K. When the temperature is higher than 279 K, the trapdoor K⁺ will be fully open and the LJM-Toth model will regress to the normal Toth model as the site accessibility is 1. For N₂, the site accessibility is 0.5 at 252 K and 1 at temperatures > 266 K. Other parameters are the same as those in the Toth model.

Supplementary Note 2: The heat of adsorption of CO₂, CH₄ and N₂ in r2KCHA

The isosteric heat of adsorption (Q_{st}) of CO₂ and CH₄ in r2KCHA was calculated by the Clapeyron equation in Equation (S4),

$$\frac{Q_{st}}{RT^2} = \left[\frac{\partial \ln P}{\partial T} \right]_q \quad (\text{S4})$$

where Q_{st} (kJ mol⁻¹) is the isosteric heat of adsorption at the loading q (mol kg⁻¹), P is the pressure (kPa), T is the temperature of the system (K), and R is the gas constant (kJ kg⁻¹ K⁻¹). If the isosteric heat is assumed to be independent of temperature, at a certain adsorption quantity, Equation (S4) can be integrated to give Equation (S5),

$$\ln P = \frac{Q_{st}}{RT} + C \quad (\text{S5})$$

where C is an integration constant. To calculate the Q_{st} , the isotherms at different temperatures were mathematically spline fitted to obtain $\ln(P)$ at a given adsorbed amount. The Q_{st} is then calculated by the slope of the linear equation of $\ln(P)$ versus $1/T$ in Equation (S5).

At the temperature range of 252 to 294 K, the N₂ adsorption in r2KCHA was strongly influenced by the trapdoor effect. The uptake was increased with the increasing temperature, disobeying the pattern of common physical adsorption. The experimentally measured N₂ uptake at these temperatures cannot reflect the real adsorption capacity due to the blocked pores. Therefore, its heat of adsorption cannot be calculated through the Clapeyron equation. The heat of adsorption of N₂ can be obtained from the fitted LJM-Toth model, as shown by the parameter Q in Supplementary Table 3.

Supplementary References:

1. Zhang J., Singh R. & Webley P. A. Alkali and alkaline-earth cation exchanged chabazite zeolites for adsorption based CO₂ capture. *Microporous Mesoporous Mater.* **111**, 478-487 (2008).
2. Zhao J., Xie K., Singh R., Xiao G., Gu Q., Zhao Q., Li G., Xiao P. & Webley P. A. Li⁺/ZSM-25 zeolite as a CO₂ capture adsorbent with high selectivity and improved adsorption kinetics, showing CO₂-induced framework expansion. *J. Phys. Chem. C* **122**, 18933-18941 (2018).
3. Toth J. State equation of the solid-gas interface layers. *Acta chim. hung.* **69**, 311-328 (1971).
4. Li G. K., Shang J., Gu Q., Awati R. V., Jensen N., Grant A., Zhang X., Sholl D. S., Liu J. Z., Webley P. A. & May E. F. Temperature-regulated guest admission and release in microporous materials. *Nat. Commun.* **8**, 15777-15786 (2017).